17th International Conference on Space Operations, Dubai, United Arab Emirates, 6 - 10 March 2023.

SpaceOps-2023, ID # 494

Experience on operations of Radio Science experiments for interplanetary missions

Jose Villalvilla[b*], Javier De Vicente[a], Peter Droll[a], Ignacio Clérigo[a], Silvano Manganelli[b], Emanuela Bordoni[a], Justin Howard[b]

[a] European Space Agency (ESA), European Space Operations Centre (ESOC), Germany

[b] Telespazio Deutschland GmbH c/o ESA/ESOC, Germany

* Corresponding author

Abstract

The joint mission BepiColombo (ESA/JAXA), currently in cruise to Mercury, hosts the MORE radio science experiment on-board the Mercury Planetary Orbiter (MPO). One of the primary scientific goals of the experiment during the cruise phase is to test the theory of general relativity, by improving the accuracy in the measurement of the gamma and beta of the parametrized post-Newtonian formalism achieved by Cassini in 2002.

Meeting MORE scientific objectives requires the use of accurate spacecraft tracking data (Doppler and range) in three different simultaneous two-way radio links (X/X, X/Ka, Ka/Ka), as well as accurate ground station and propagation media calibrations. In order to meet such needs, ESA DSA3 station in Malargüe (Argentina) has been upgraded for radio science support over the last years according to a development and deployment roadmap and has played a pivotal role in the radio science campaigns performed so far (Superior Solar Conjunctions in March 21 and February 22). Unprecedented valuable results have been obtained so far, and further results are expected as part of the remaining campaigns, which will extend until the end of 2025.

The use of various novel techniques, the operation of the Ka-band links and the stringent requirements in terms of accuracy and stability have made radio science related operations particularly challenging. This article describes the context of the experiment, the experience gained during preparatory in-flight testing, and the support given to the first two radio science campaigns (31 operational passes) from DSA3. Main critical aspects (in particular related to the operation of Ka-links) are described, as well as the lessons learned for future radio science supports (BepiColombo and JUICE missions).

Keywords: Radio science, Ka-band, BepiColombo, pointing, troposphere

1. Introduction

ESA operates its interplanetary missions from the European Space Operations Centre (ESOC), located in Darmstadt, Germany. To communicate with spacecraft, ESOC makes use of ESA's tracking station network (ESTRACK), which is comprised of several terminals around the world for the tracking of Near Earth and Deep Space missions. For the latter, a network of 35-m antennae located in New Norcia (DSA-1, Western Australia), Cebreros (DSA-2, Spain) and Malargüe (DSA-3, Argentina) is used.

In recent years, one driver for the evolution of ESTRACK's deep space network has been the support to radio science experiments. The MORE and 3GM experiments, on-boarded in the BepiColombo and JUICE missions respectively, rely on an extremely accurate tracking system for both integrated Doppler and ranging observables, with a performance that is one order of magnitude better than what is available with current tracking systems.

DSA-3 is ESTRACK's first deep space antenna equipped for full radio science support [1]. The provisions made during the design phase of DSA-3 for later radio science upgrades have facilitated a smooth implementation of the new capability.

This paper describes the ground station preparatory activities in DSA-3 prior the first radio science campaigns (SCE#1 in March 2021 and SCE#2 in February 2022), the analysis of the results from these measurements and the experience gained during the ground operations. The paper is structured as follows:

- Section 2: Overview of test and operational campaigns
- Section 3: Results - Inspection and analysis of Data
- Section 4: Corrective actions
- Section 5: Discussion and future work
- Section 6: Conclusion

1.1 *MORE radio science experiment*

The main scientific goals of MORE (Mercury Orbiter Radio science Experiment), the radio science experiment on-board BepiColombo, span in the fields of geodesy, geophysics and fundamental physics, including the determination of Mercury's gravity field, its surface properties, but also the internal structure of the planet and its rotational state (obliquity and librations amplitude). Also, the frequent exposition of the Spacecraft to superior solar conjunction geometries (i.e. where the Sun lies between the Earth-probe line of sight) will allow other fundamental physics goals like the measurement of relativistic post-newtonian parameters γ, controlling the deflection of light and the time delay of ranging signals [1].

This experiment relies on the use of extremely precise tracking systems, able to provide unprecedented tracking accuracy as result of the exploitation of multi-frequency links (X/X, X/Ka and Ka/Ka simultaneously), in combination with dedicated measures on both ground and space segments. For the latter, the use of an on-board accelerometer and other self-calibration means allow an accurate measurement of on-board delays. MORE makes use of a dedicated transponder (KaT, Ka translator) for the Ka/Ka-band link.

MORE was one of the experiments on-board BepiColombo exercised during the cruise phase, as its use was already required at the time of the first Solar Conjunctions in 2021 (SCE#1) and 2022 (SCE#2). The mission plan for the experiment foresees the utilisation of as many superior solar conjunction opportunities as possible during the BepiColombo cruise, lasting until late 2025 with the capture of the probe by Mercury's gravity field. The remaining goals of MORE will be fulfilled during the nominal one year BepiColombo mission around Mercury, in 2026.

1.2 *Radio science capability in Deep Space Antenna 3 (Malargüe, Argentina)*

The implementation of the triple link capability (X/X, X/Ka, Ka/Ka)[*] needed for MORE and 3GM, which allows for cancellation of solar plasma effects, has required several upgrades at DSA-3. A 100W Ka-band SSPA, dedicated Ka-band frequency conversion equipment, a mechanism correcting the squint between receive and transmit beam at Ka-band and dedicated wideband pseudo-noise regenerative signal structures (at 3 and 24 Mcps) are part of these upgrades. Dedicated line-of sight tropospheric calibration equipment has been additionally developed and installed on-site [2].

[*] Ka downlink frequencies are different between X/Ka and Ka/Ka links, as each Ka downlink is coherent with a different uplink

2. Test and operational campaigns

Following the deployment of the new radio science capability in DSA-3 and the launch of BepiColombo in October 2018, several test campaigns have been carried out in order to verify the readiness of the system, exercise the operations and optimise the configuration. These campaigns are summarised in Table 1.

Table 1. Major MORE radio science operational activities and campaigns until SCE#2

Dates	Id	Description/Comments
09.12.2018	MORE commissioning	Functional test following the BepiColombo LEOP
02.05.2019 – 29.05.2019	Triple-link	13 tracking passes over DS3 exercising the triple link. The opportunity was also used for TDCS validation. Some passes affected by strong wind.
31.01.2020	--	Nominal pass, i.e. no Ka-band uplink issues and stable AGC in the three Ka-band links. Uncorrected pointing error (stellar aberration + beam squint) ~11.6 mdeg. (More detail for Triple-link campaign, including motivation and main outcome is given in appendix A).
03.09.2020 – 15.09.2020 (part I) 04.11.2020 – 26.11.2020 (part II)	RSE E2E	Test campaign formally included in the MORE test plan. Full functional test of the complete tracking system. The most important test goals were: - Calibration of KaT and DST group delay and phase delay - Generation of Doppler and range observables - Test of multi-link plasma calibration - Assessment of the stability of residuals - First operational usage of Ka/Ka on-line calibration
04.02.2021	Test slot #1	First opportunity to validate stellar aberration correction in the orbital predictions. Beam squint correction could not be validated due a HW problem in the M8/M12 positioner. Uncorrected beam squint angle ~11.6 mdeg.
06.02.2021	Test slot #2	Second opportunity to confirm stellar aberration correction. The root cause of HW issues in M8/M12 was identified (cabling) and fix and beam squint correction was tested.
13.02.2021	Test slot #3	Operational pass, last part dedicated to the optimization of beam squint correction. The corrected pointing error was ~25mdeg (beam squint) + TBD (stellar aberration). First operational usage of TDCS
26.02.2021	Dress rehearsal + Test slot #4	First part of the pass: exercise the system in preparation for SCE#1, second part: confident test on the correction of stellar aberration and beam squint (~27.4 mdeg)
10.03.2021 – 24.03.2021	**SCE#1**	**First operational campaign during Superior Solar Conjunction, minimum SEP 1.18 deg**
15.04.2021- 08.06.2021	Test passes type #1	Passes including a 10 min. conical scan every hour. Reduced scan radius in order to avoid any impact on X-band comms
29.04.2021	Test pass type #3	Test pass dedicated to Ka-band transmit pointing issues. Beam squint ~ 23.1 mdeg
01.12.2021	Test pass type #3	Test pass dedicated to Ka-band transmit pointing issues. Beam squint ~ 19.6 mdeg
13.01.2022	Dress rehearsal	
29.01.2022 - 12.02.2022	**SCE#2**	**Second operational campaign during Superior Solar Conjunction, minimum SEP 2.07 deg**

3. Results: Inspection and Analysis of Data

3.1 *End-to-End test campaign*

The ultimate goal of the end-to-end test campaign was to verify the full functionality of the complete tracking system in final configuration, i.e. the triple-link, the TDCS (which at the time was still in its validation phase) and the on-board gravitational accelerometer. A summary of the main findings is given in Table 2.

Table 2. Main operational issues/open points during end-to-end campaign

PN ranging in Ka/Ka	Failed acquisition. The root cause was found on the ground receiver software where a 32-bit register overflows at clock offsets corresponding to RR values larger than 16 Km/s. This limit was exceeded during the campaign.
Received power (onboard)	Unstable behaviour of the KaT coherent AGC during (Ka-band uplink).
Carrier unlocks (onboard)	On-board PN 24 Mcps ranging receiver (Ka-band uplink) unlocked shortly in several occasions.
PN unlocks (on-board)	On-board receiver unlocked from the Ka-band uplink carrier in several occasions.

The investigation of the above issues started with the inspection of data from the relevant passes. The data from the ground station and the spacecraft housekeeping were graphically presented together in the same timeline (after proper alignment of Earth and Spacecraft times due to one way travel light time from the spacecraft).

The example given in Fig.1 (first part of the pass on DOY329, low elevation) shows unstable on-board carrier and ranging AGC (Ka-band uplink) levels. Carrier AGC levels varied from 79 to 257 (transponder engineering values corresponding to -118dBm and -127dBm respectively) in the case of the carrier, with one peak at 571 (-137 dBm). A total of ten on-board ranging unlock events (chip and/or code) are observed, although in this example, there were no carrier unlocks, as in the case of other passes. The very stable output power observed for the ground station Ka amplifier (<0.15 dBpk-pk) is not compatible with the high variability in the on-board AGCs. On the downlink side, AGC (Ka-band downlink, TM & RSE) variations of around 6 dBpk-pk in RSE and 3dB dBpk-pk in TM were observed. The similar magnitude of the rapid variations seen on carrier level and Es/No indicates signal attenuation and no noise increase, thus suggesting the presence of scintillation and/or pointing losses. It is worth to remark that the slow component of this variation can be attributed to the decrease of sky noise (due to gases and liquid) as the elevation increases.

For what regards weather conditions, the atmospheric attenuation (as measured by the TDCS in the line-of-sight) was a bit unstable but low. The wind speed remained below 12.5 m/s, albeit with high variability at the start of pass.

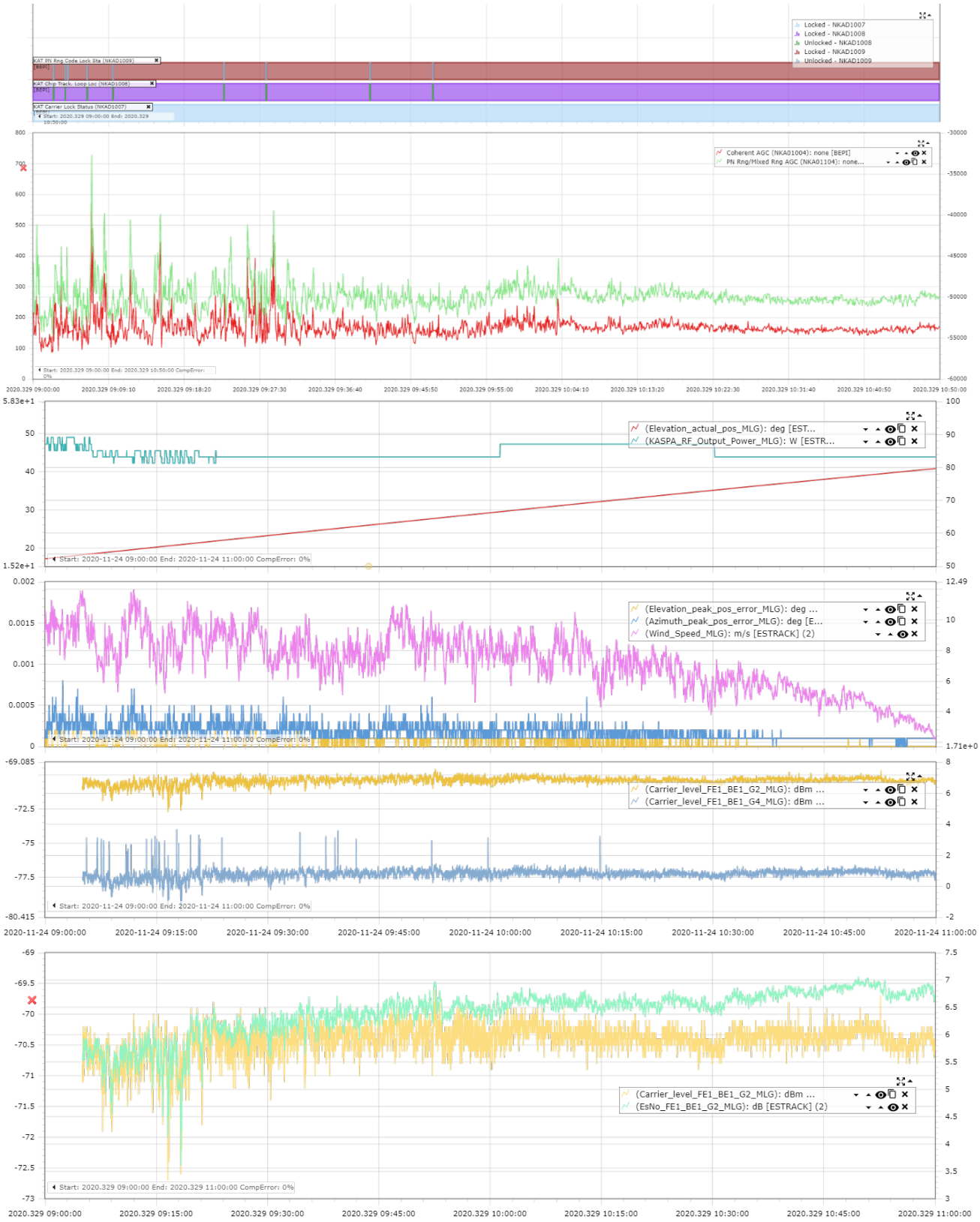

Fig. 1. Pass DOY 329 (relevant part) on-board data (top) and on-ground data (bottom) – Credits: BepiColombo and ESTRACK

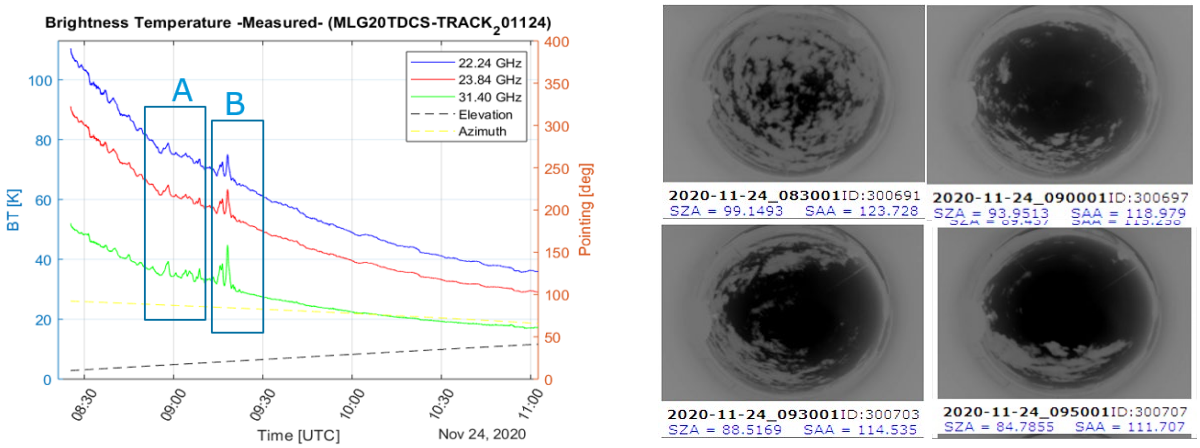

Fig. 2. Pass DOY 329 additional on-ground data: TDCS brightness temperature (left) and cloud camera images (right)

The brightness temperature measured by the TDCS (see A and B events in Fig.2) hints at the presence of clouds passing by the line-of-sight, which involve rapid spatial variations of water vapour and liquid water and can translate into turbulence. The wind reported in Fig.1 is also indicating possible turbulence at the relevant tropospheric layer and thus amplitude scintillation (enhancements and fades of attenuation). The cloud camera reveals the presence of clouds at the beginning of the pass, then dispersing, in line with the TDCS measurement.

The assessment performed following this campaign hinted at tropospheric scintillation effects being a major cause of many of the power drops experienced in the Ka links. It also highlighted two issues related to the beam squint correction mechanism, one due to missing tailoring on the Station Computer (STC), the other resulting from an incorrect calculation routine in the Front-End Controller (FEC). Beam squint during the campaign (7.1 mdeg on DOY329) still allowed to track without beam squint correction but was starting to become significant.

Furthermore, ESOC Flight Dynamics (FD) confirmed that stellar aberration was at the time not corrected in the delivered Tropospheric Data Messages (STDM), as this led to adverse effects in the derivation of topocentric quantities needed by the ground station modem to compensate for the Doppler effect. This effect alone was responsible for a 4.5 mdeg pointing error on DOY329.

All issues related to beam squint and stellar aberration were fixed after the campaign. Their combined effect (estimated at 11.6 mdeg) could however not explain the rapid variabilities that had been observed (wind and tropospheric effects were suspected to account for the rest). Specific actions were defined to improve pointing prior to Solar Conjunction Experiment (SCE) #1, MORE's first operational and scientific campaign.

3.2 Solar Conjunction Experiment #1 (Mar. 2021)

The campaign was relatively uneventful, with the exception of the first pass (DOY069), when short unlock events of the on-board PN ranging signal were observed (Fig.3, top plot). A significant correlation can be seen on this day between the on-board PN ranging unlocks and Ka-band uplink level drops, ground station pointing error in azimuth (as reported by the antenna servo encoder†), and wind speed.

† Conversion from azimuth to cross-elevation allows a better insight of the true pointing error.

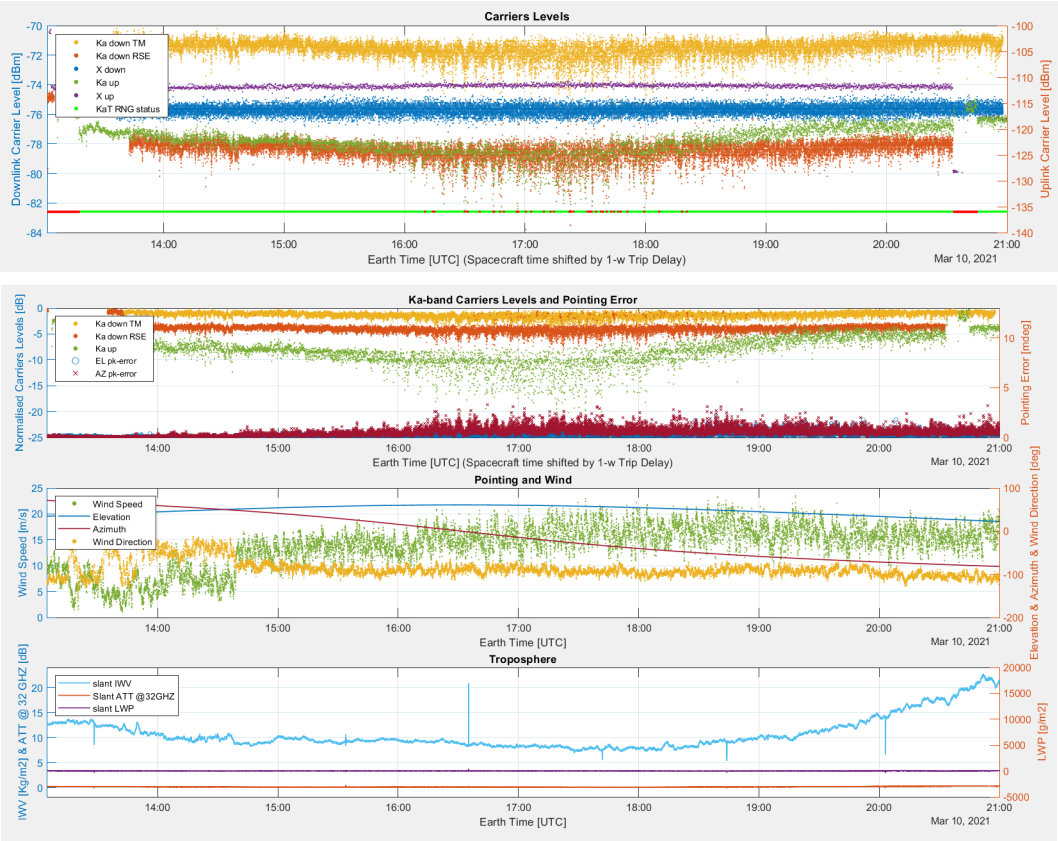

Fig. 3. Ground and Spacecraft data from first day of SCE#1 (pass on DOY 069)

Fig.4 shows the phase stability of the Ka/Ka link at the station, which is recorded during the pass (thus simultaneously to radiometric measurements on the spacecraft) by means of a dedicated station calibration loop. This recording is also a deliverable to the MORE team, considered the calibration of instabilities caused by ground station equipment.

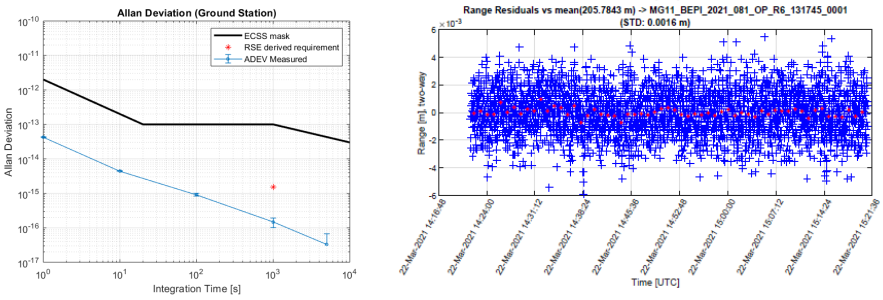

Fig. 4. Ground station (Ka Tx/Ka Rx) stability (pass on DOY 081) – ADEV (left) and range residuals (right)

3.3 Solar Conjunction Experiment #2 (Jan.-Feb.2022)

An optimisation of the beam squint mechanism (use of new mirror correction coefficients [3]) was implemented prior to this campaign (see section 4) to improve Ka pointing further. The analysis of the data and logs recorded showed a clear correlation between signal fluctuation (found to be slightly higher in the uplink than in the downlink) with wind and tropospheric effects (sometimes separately, sometimes combinedly). A small and slow systematic signal loss vs elevation was also observed.

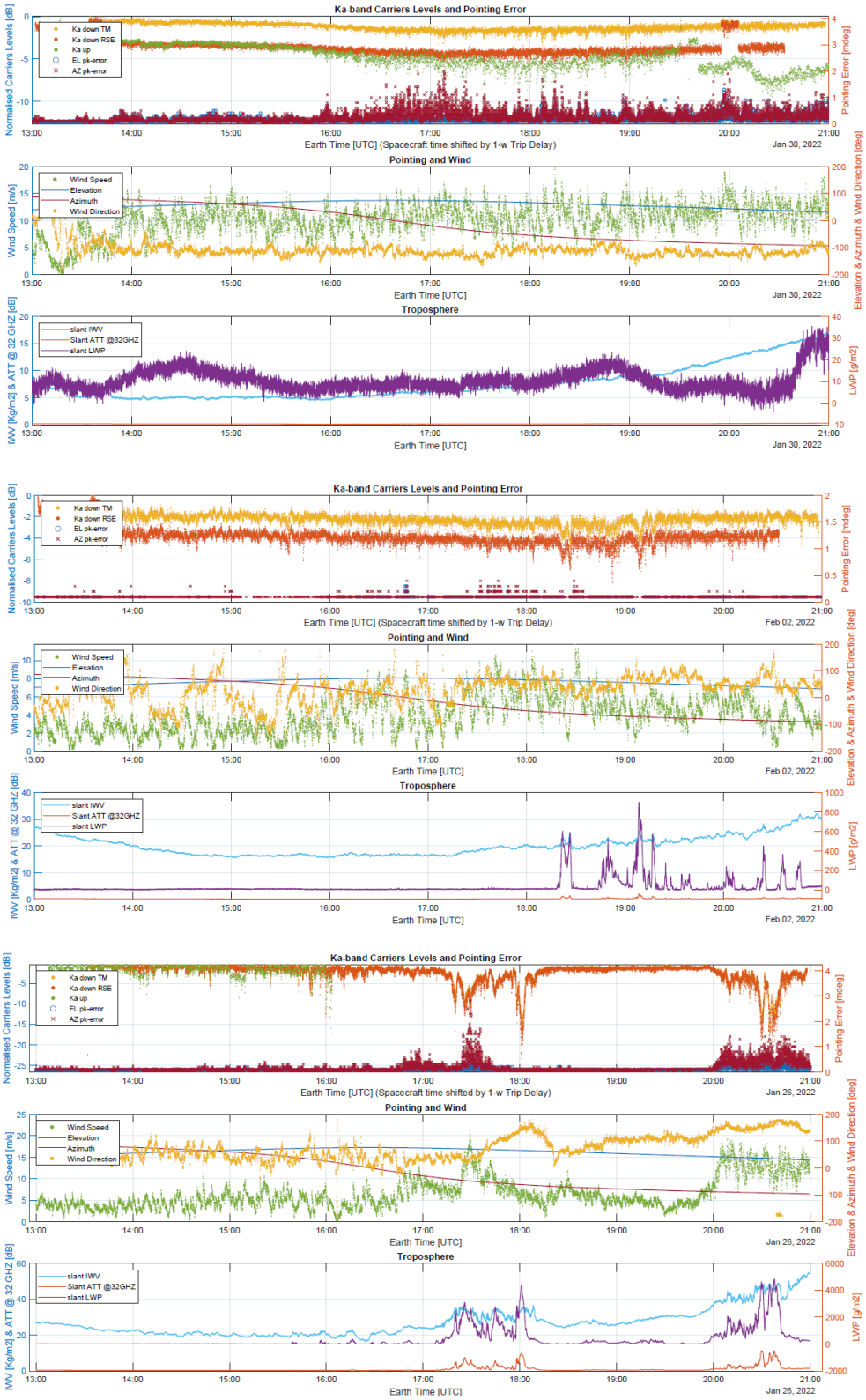

Fig 5. DOY030 (1st triplet), DOY033 (2nd triplet) and DOY026 (3rd triplet) data, showing correlation between signal fluctuations with wind only (DOY030), liquid water only (DOY033), and combined wind, water vapour and liquid water (DOY026)

4. Corrective actions and validation

4.1. Corrective actions

Stellar aberration

This phenomenon is produced by the motion of the observer (ground station in Earth) around the Sun, which changes the apparent direction of an observed celestial from the true direction. Its correction depends upon the component of the ground antenna's inertial velocity perpendicular to the line-of-sight of the spacecraft. The Earth's velocity relative to the Solar System Barycentre (SSB) is around 30 km/s, leading to a maximum error in the pointing of about 5.7 mdeg (significant for Ka-band).

ESOC FD provides orbital predictions by means of STDM files. These files contain geocentric state vectors that can be converted at each station to generate pointing (antenna) as well as range and range-rate predicts (receiver). Originally (e.g. prior to the need to support ka/ka links) STDMs could correct for stellar aberration, although this came at the cost of a certain error in range and range-rate quantities. Since the effect of stellar aberration is negligible for X-band links (due to the larger antenna beamwidth), stellar aberration correction information was at the time disabled. This changed when Ka operations started, and required the implementation of a more precise algorithm, which allowed stellar aberration corrections and minimised range and range-rate errors.

Rx-Tx beam squint (also known as light time correction)

The light-time correction takes into account the offset between the transmit and receive beams due to distant spacecraft moving across the line of sight. It was therefore necessary to modify the interplanetary STDM format to add besides the vector for the receive beam pointing also a vector for the transmit beam pointing.

The optical design of DSA-3 [3] allows the compensation of the Ka-band Rx-Tx beam squint up to 40 mdeg by means of two moveable beam waveguide (BWG) mirrors, each tiltable in 2 axes (M8 and M12) as shown in Fig.6 (left). Whereas the absolute value of the Rx-Tx beam squint remains quasi-constant for several days, these mirrors move continuously during a pass and take into account the antenna rotation in Azimuth and Elevation. The generation of the Ka-band Rx-Tx squint results in a gain loss of the Ka transmit BWG path. Due to the selected optical design, this gain loss is asymmetric (confirmed by predictions and measurements) with respect to the Rx-Tx offset (Fig.6, right). An upper bound for the losses can be estimated by ΔG [dB] = -0.003 * (Rx-Tx Offset [mdeg])2. Further work in this domain is required to reduce the gain loss by considering the asymmetry in the compensation algorithm.

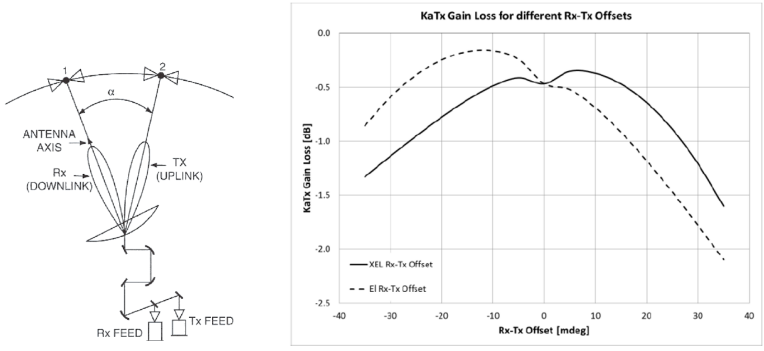

Fig. 6. Beam squint: illustration of beam squint (left) and predicted gain loss vs. Rx-Tx offsets for position 40/40 deg (azimuth/elevation) [3]

The beam squint correction capability was already available at DSA-3 before the preparation and beginning of the support to the MORE experiment. However, the capability was neither optimised (by using improved coefficients) nor

tailored in the STC at the time of the early MORE campaigns, which contributed to the issues described in previous sections.

4.2. Validation

Dedicated pointing tests were organised with the BepiColombo mission team to validate the various fixes, ensuring no impact to routine X-band communications. The validation of the stellar aberration fix was performed by comparing performance with and without stellar aberration corrections (two sets of orbital predictions were prepared for this purpose). The antenna pointing error was estimated by performing a conical scan and measuring the sum channel of the Ka-band telemetry downlink.

The Rx-Tx beam squint correction was validated by applying elevation and cross-elevation offsets on top of the beam squint correction (Fig.7) in order to determine the peak and potential asymmetries of the beam. The signal level measured by the Ka-band on-board receiver was used for this purpose.

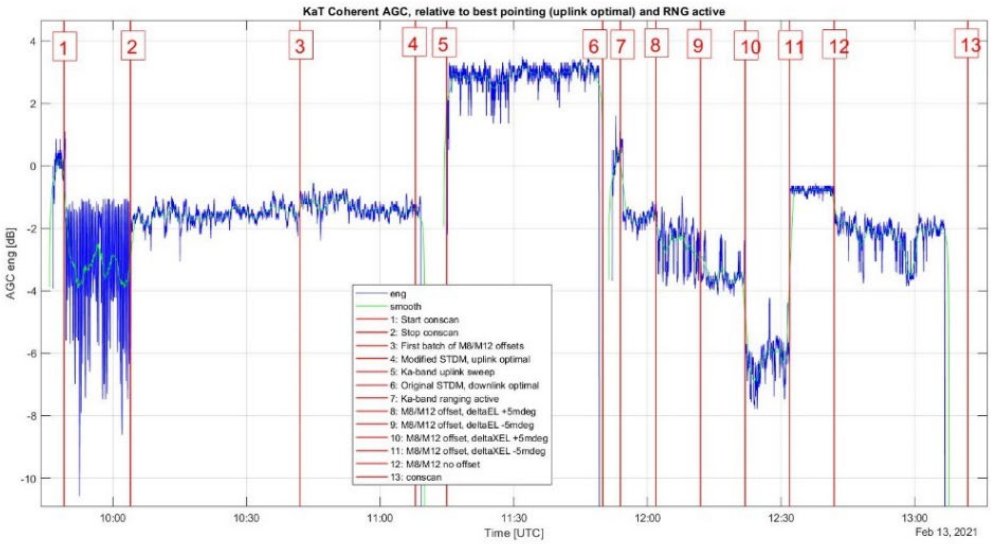

Fig. 7 On-board AGC levels (relative) during Ka-band pointing tests

In a second step, a dedicated test campaign was organised prior to SCE#2. This campaign consisted of three tests, which are summarised in Table 3.

Table 3. Pointing test types prior to SCE#2

	Objectives – Description	Requirements
Ka Downlink (Test type #1)	Pointing refinement – Fully automated Ka-Band conscan tests on Ka-TM and radiostars.	Ka TM, KaT off
Ka Tx verification (Test type #2)	Optimisation of Systematic Pointing Error Model (SPEM) coefficients - Pointing at radiostars using the Ka-band transmit feed in reception covering Rx/Tx squints up to 20 mdeg.	No need for link to BepiColombo
Ka Tx/Rx tests (Test type #3)	Optimisation of Systematic Pointing Error (SPEM) coefficients	Ka TM on, KaT on

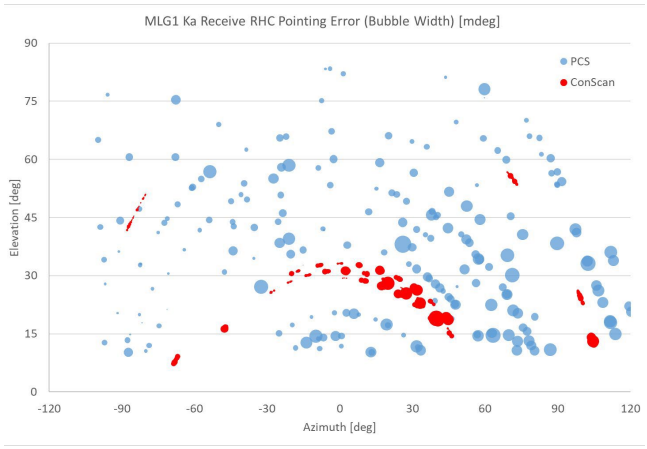

ConScan: 0.9/4.6/0.8 mdeg (avg/max/stdev) – RadioStar: 2.3/5.2/1.0 mdeg (avg/max/stdev)

Fig. 8. Combined results of tests type #1: Hemisphere coverage of Con-scan measurements with BepiColombo (Ka-TM downlink) and radio star measurements (Test type #1). Bubble width corresponds to the measured pointing error.

Results of test types #1 and #3 are shown in Fig.8 and Fig.9 respectively. For the latter, SPEM coefficients were turned on and off during the pass and the on-board level reported by KaT's AGC recorded. The results not only showed an improvement of the on-board AGC level of 0.5 dB, but also confirmed smaller signal variations on-board when SPEM coefficients were used.

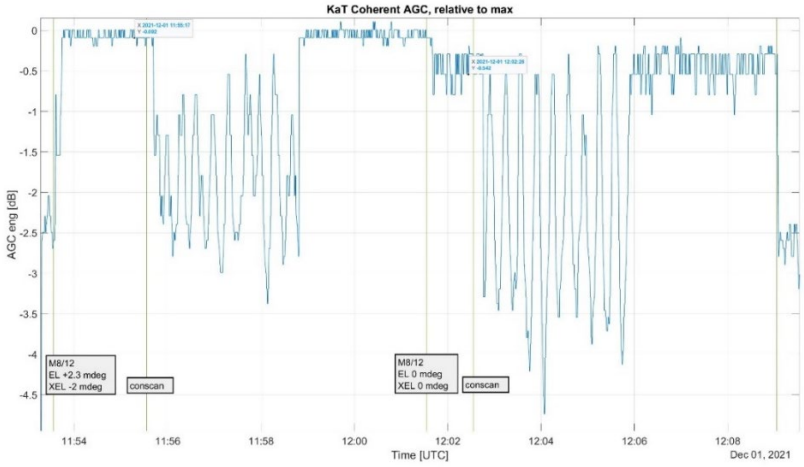

Fig. 9. Results of tests type #3: on-board AGC levels (relative)

Applying the new set of coefficients, a reduction of the maximum error from 6.5 to 4.5. mdeg was possible, resulting in lower average losses as well as a reduced sensitivity to additional superimposed pointing error (e.g. mechanical noise caused by wind). Based on these results, SPEM coefficients were adopted subsequently for future campaigns.

5. Discussion and future work

The corrective actions described in this work have resulted in a significant improvement of Ka transmit beam pointing performance. The influence of troposphere, which cannot be mitigated, requires further investigation to characterise its effect and verify current available models. The climatic particularities of Malargüe (e.g. occasional humid and warm weather after summer storms) constitutes an interesting study case due to the large tropospheric

scintillation at high frequencies. Under these conditions (i.e. high day-night temperature variation and significant amounts of moisture in the soil) the convective currents of warm wet air rising from the soil can lead to turbulence.

The data analysis performed in this paper shows that the signal fluctuations caused by scintillation are larger in the case of the uplink, which should also be a matter of further study. The perturbation caused by the turbulent layer of the troposphere (last kms closest to Earth) on a flat wavefront results in a corrugated wavefront. The effect on the signal should be different depending on whether the perturbation is located close to the transmitter (uplink) or the receiver (downlink). In the first case, the corrugation in the wavefront might be amplified as it propagates further away.

This paper has highlighted the challenges for simultaneous Ka-band uplink and downlink operation. In addition to the implementations described up to this point, additional work has taken place in specific areas or is expected in the future, for both Ka-band operation and radio science support. Already performed work includes the analysis of the accuracy and stability of station calibration loops, which has led to a recommendation to adopt the station's medium loop (ground station equipment only, no beam waveguide) in favour of the long loop (up to the main reflector) for station calibrations in all bands. The electromagnetic simulations performed as part of this analysis have determined accurately the delay in the beam waveguide system, allowing a straightforward conversion from medium loop data to the reference point used by Flight Dynamics for the evaluation of radiometric measurements. Medium loop calibration results have been described in section 3 for the Ka/Ka case.

Future work foresees the use of monopulse autotrack for the Ka-band downlink as well as the detailed assessment of the impact of Ka-band transmit interference on the X-band downlink. For the first, the asymmetric beam at Ka-band transmit results in a distinctly higher sensitivity to pointing offsets than initially expected, which could be mitigated with the use of monopulse autotrack in open loop tracking. For the latter, latest test results indicate the presence of unwanted incoming Ka-band transmit energy reaching the X-band feed for certain positions of the M8 and M12 mirrors. A detailed analysis of signal fluctuations using Artificial Intelligence techniques is also an area of future study.

6. Conclusions

This paper describes the preparation and execution of the first BepiColombo radio science campaigns (SCE#1 and SCE#2), with main focus on pointing performance in Ka band. Following the work in this and other areas [1], ESA's DSA-3 station, which allows fully automated operation for radio science supports, has become a state-of-the-art asset for the operation of radio science experiments on-boarded in deep space missions. In addition to the current support to BepiColombo's radio science, DSA-3 will also be a crucial element for the radio science experiments on-boarded in the JUICE mission.

Acknowledgements

The authors would like to thank the MORE team, Frank Budnik and Gabriele Bellei from ESOC FD, Fabio Pelorossi (Ground Station Engineering) and Michel Dugast (DSA-3 station engineer).

References

[1] The implementation of a radio-science capability in the ESA deep space network of antennae, de Vicente J. et al, ESA TT&C 2019

[2] Tropospheric Delay Calibration System (TDCS): design and performances of a new generation of microwave radiometers for ESA deep space ground stations, Lasagni-Manghi R. et al, ESA TT&C 2019

[3] Performance of the Ka-Tx Beam Steering Approach of DSA3, Droll P. et al, Proceedings ESA TT&C 2016

[4] DSA-3 – The 3rd ESA Deep Space Station in Malargüe, Argentina, Maddè, R. et al, ESA TT&C 2013